



Title	Mechanism of droplet generation and optical emission of metal atoms in atmospheric-pressure dc glow discharge employing liquid cathode
Author(s)	Shirai, Naoki; Suga, Goju; Sasaki, Koichi
Citation	Plasma Sources Science and Technology, 29(2), 025007 https://doi.org/10.1088/1361-6595/ab6abc
Issue Date	2020-02-06
Doc URL	http://hdl.handle.net/2115/80375
Rights	This is a peer-reviewed, un-copyedited version of an article accepted for publication/published in Plasma Sources Science and Technology. IOP Publishing Ltd is not responsible for any errors or omissions in this version of the manuscript or any version derived from it. The Version of Record is available online at https://doi.org/10.1088/1361-6595/ab6abc .
Type	article (author version)
File Information	Shirai_revised.pdf



[Instructions for use](#)

Mechanism of droplet generation and optical emission of metal atoms in atmospheric-pressure dc glow discharge employing liquid cathode

Naoki Shirai

Hokkaido University, Japan

E-mail: nshirai@qe.eng.hokudai.ac.jp

Goju Suga

Hokkaido University, Japan

Koichi Sasaki

Hokkaido University, Japan

E-mail: sasaki@qe.eng.hokudai.ac.jp

Abstract.

The mechanism of the droplet generation and the optical emission of metal atoms in an atmospheric-pressure dc glow discharge employing an electrolyte cathode were investigated experimentally. We examined the correlation among the dynamics of the electrolyte surface, the density and its spatial distribution of gas-phase droplets, and the optical emission intensity in an atmospheric-pressure dc glow discharge employing an electrolyte cathode. The experimental results reveal the following mechanism for the droplet generation and the optical emission of metal atoms. The correlation between the droplet density and the optical emission intensity indicates the importance of droplets in the transport of metal atoms from the electrolyte to the gas phase. The production of metal atoms from droplets seems to be a mechanism of the optical emission. We propose two mechanisms for the generation of droplets from the electrolyte cathode. The first is the distortion in the shape of the electrolyte surface. Droplets are produced from the tip of the cone-shaped electrolyte surface via a process similar to electrospray. The first mechanism works for the initiation of the droplet generation in the early stage in the temporal evolution of the discharge. The second mechanism is the explosive reaction between Na particulates and water. We speculate that Na particulates are produced from Na atoms in the gas phase. Once the second mechanism is switched on, the self-sustained productions Na atoms, Na particulates, and NaCl droplets are realized, resulting in the intense optical emission of metal atoms.

PACS numbers: 52.25, 52.50, 52.80, 79.60

Keywords: atmospheric-pressure plasma, plasma-liquid interaction, droplet, optical emission spectroscopy

Submitted to: *Plasma Sources Sci. Technol.*

1. Introduction

Atmospheric-pressure plasmas in contact with liquids have been investigated in all over the world because of their potential applications [1–3]. For example, in the field of nuclear fusion research, the plasma-liquid interaction attracts much attention in conjunction with the development of a liquid-metal diverter system [4]. Another typical plasma in contact with liquid is an atmospheric-pressure discharge with a liquid electrolyte electrode. This is a plasma produced by applying a high voltage between an electrolyte and a metal electrode. Plasmas with liquid electrodes have been studied for a long time before the middle of 20th century [5–7]. In 1990s, Cserfalvi *et al.* reported the utilization of the optical emission from a liquid-electrode plasma for the element analysis in the liquid [8–10]. After 2000s, there are some publications which report optical emission spectra of liquid-electrode plasmas [11–17]. Recently, the liquid-electrode plasma is focused from the point of view of applications such as surface treatment, sterilization of water, and nanoparticles synthesis [18–26].

In previous papers, we reported several types of atmospheric-pressure glow discharges using liquid electrolyte electrodes and helium flow [27–37]. We showed that the optical emission of Na was observed from the plasma when a NaCl solution worked as the cathode of the discharge [27–31]. The optical emission intensity of Na was dependent on the concentration and the temperature of the NaCl solution [27, 28]. In addition to our works, there are many papers which report the optical emissions of metal atoms which are dissolved in cathode solutions [11–16, 38–44]. The optical emission of metal atoms indicates the transport of dissolved (or ionized) metal atoms in the solution to the gas-phase of the plasma. The authors of the above literature discuss sputtering of cathode electrolyte, thermal evaporation, and phenomena similar to electrospray as the mechanism for the transport of metal atoms from the solution to the plasma. However, the detailed mechanism for the transport of metal atoms has not been clarified yet. On the other hand, in the element analysis of a liquid sample by inductively coupled plasma atomic emission spectroscopy, mist, which is generated from liquid using a nebulizer, is introduced into the plasma to induce the optical emission [45]. If mist or the droplet of the electrode liquid is generated by the plasma-liquid interaction, it can be a mechanism for the transport and the optical emission of metal atoms. Previously we confirmed that the droplet ejection from the liquid surface was observed only when the liquid worked as the cathode [27, 28].

This study focuses on the ejection of droplets from the liquid surface by the plasma-liquid interaction. We investigated the ejection processes of droplets using a color high-speed camera and laser Mie scattering. In addition, we examined the dependence of the NaCl concentration on the optical emission intensity of Na. We believe that the results are helpful for understanding the mechanism of the transport of metal atoms

from the solution to the plasma. Supplementary data including movie files are available at stacks.iop.org/PSST/XX/XXXXX/mmedia.

2. Experimental procedure

Figure 1 shows the experimental setup of the electrolyte-cathode discharge with a helium flow. The concentration of NaCl in the electrolyte cathode was 0%-10%. The electrolyte was at room temperature (approximately 25 °C). The stainless-steel nozzle anode had inner and outer diameters of 500 and 800 μm , respectively. The distance between the tip of the anode and the electrolyte surface was 0.5-10 mm. Helium gas was fed toward the electrolyte surface from the nozzle anode in the air. The gas flow rate was adjusted at 200 sccm using a mass flow controller. A glow discharge was generated by applying a dc voltage between the nozzle anode and the electrolyte. The dc voltage was applied using a regulated dc power supply (Matsusada HAR-5P120) in the constant-current mode. The discharge current was varied up to 120 mA. A ballast resistor of 100 k Ω was connected in series with the nozzle anode. The electrolyte cathode was electrically grounded via a platinum wire immersed in the electrolyte and a 100 Ω resistor. The discharge current was measured by recording the voltage drop at the 100 Ω resistor. The voltage between the anode and the electrolyte was measured using a high-voltage probe (Tektronix P6015A).

The visible-light image of the discharge was taken using a consumer-grade digital camera (Olympuse Pen) combined with a macro lens. Optical emission spectroscopy was conducted using a spectrograph (Ocean Optis USB2000+). To visualize small droplets, we adopted laser Mie scattering employing a He-Ne laser at a wavelength of 623 nm. The output power of the He-Ne laser was 5 mW. The diameter of the laser beam was expanded to a similar size to the distance between the electrodes using two lenses. We placed a band-pass filter with transmissions at the laser wavelength and a wavelength shorter than 500 nm in front of the digital camera in the laser Mie scattering experiment. The temporal evolutions of the optical emission image and the shape of the electrolyte surface were observed using a color high-speed camera (Nac HX-7S) with a frame rate of 10⁵ fps.

3. Results

3.1. Visualization of droplet generation

Figure 2 shows images of laser Mie scattering observed at various discharge conditions. In these figures, the area with droplets are indicated by red which is caused by the Mie scattering of the He-Ne laser beam. The blue positive column is due to the transmission of the band-pass filter below 500 nm. When tap water was used as the cathode, we never observed droplets, as shown in Fig. 2(a). When an NaCl solution with a concentration of 1% was used as the cathode, we observed the generation of droplets, as shown in Fig. 2(b). The droplets seemed to be ejected toward the upward

direction from the solution surface. Similar phenomena were observed by Hieftje and coworkers [39]. When the concentration of NaCl was increased to 5%, as shown in Fig. 2(c), we observed the increase in the amount of droplets considerably. We observed the expansion of the area with droplets toward the higher distance from the solution surface. In addition, as shown in Fig. 2(d), the droplets also spread their existence area in the radial direction. The movie file of the same data as that shown in Fig. 2(d) is available at stacks.iop.org/PSST/XX/XXXXX/mmedia. (See the file of movie file spp1.mp4.) Figure 2(e) shows the Mie scattering image when the NaCl solution worked as the anode of the discharge. As shown in the figure, we observed no droplets in the solution-anode discharge.

3.2. Correlation between amount of droplets and optical emission intensity of metal atoms

As described in the previous section, the number of droplets increased with the concentration of NaCl. On the other hand, as reported in our previous papers [27, 28], we observed the increase in the optical emission intensity of Na with the concentration of NaCl. In this paper, we show another experimental result of the optical emission which was observed when we used the mixed solution of NaCl and CuSO₄ as the cathode of the discharge. Figure 3(a) shows the image of the optical emission when a pure CuSO₄ solution was used as the cathode. We observed the green optical emission from the plasma. The green optical emission came from the electronic excited states of Cu, indicating a similar process to that observed in the NaCl solution. We observed droplets in the discharge shown in Fig. 3(a), but the number of droplets was much smaller than that shown in Figs. 2(b)-2(d). When we added NaCl into the CuSO₄ solution, we observed a remarkable increase in the optical emission intensity of Cu as shown in Figs. 3(b) and 3(c). In these figures, the optical emission of Cu inside and around the plasma column was masked by the optical emission of Na (the orange color), and the optical emission of Cu was observed at a long radial distance from the plasma column.

Figure 4 shows the optical emission spectra observed in pure CuSO₄ solution and a mixed solution of CuSO₄ and NaCl. The optical emission intensity of Cu was clearly increased by the addition of NaCl into the CuSO₄ solution. The number of droplets was also enhanced by the addition of NaCl, as shown in Fig. 2. These experimental results indicate a positive correlation between the number of droplets and the optical emission intensity of metal atoms. The optical emission intensities of Na and Cu were negligible in the solution-anode discharge, which also correlated with the negligible number of droplets, even when the discharge current was increased.

3.3. Temporal variation in optical emission image of Na

Figure 5 shows the temporal variation in the optical emission image of the discharge employing an NaCl solution as the cathode after ignition. The movie file of the same data as that shown in Fig. 5 is available at stacks.iop.org/PSST/XX/XXXXX/mmedia. (See

the file of movie file spp2.mp4.) At 10 μs after the ignition, we observed the formation of the discharge channel between the needle anode and the NaCl solution (the cathode), as shown in Fig. 5(b). After that, we observed the shortening of the bright discharge channel (Fig. 5(c) and Fig. 5(d)). The optical emission of Na was firstly observed at 320 μs after the ignition (Fig. 5(e)). The first optical emission of Na was localized, and the region with the optical emission had a spot on the solution surface. The shape of the optical emission of Na suggests a phenomenon which is similar to a firing from the spot. The number of the spot on the solution surface increased with time (Figs. 5(f)-Fig. 5(i)), resulting in the spread region with the optical emission of Na, as shown in Fig. 5(j). The ejection of droplets was observed after 600 μs after the ignition of the discharge, as shown in Figs. 5(k) and 5(l), where a part of droplets is seen as black points in the discharge space.

3.4. Temporal change in shape of solution surface

To observe the shape of the solution surface, we illuminated the surface using a halogen lamp and took the high-speed movie from the upper oblique direction. Figure 6 shows the temporal change in the shape of the solution surface after the ignition of the discharge. The movie file of the same data as that shown in Fig. 6 is available at stacks.iop.org/PSST/XX/XXXXX/mmedia. (See the file of movie file spp3.mp4.) As shown in the figure, we observed the perturbation on the solution surface in the time between the ignition and the initiation of the optical emission of Na. The perturbation on the solution surface contained the formation of several cones which are indicated by arrows in the figure. It was clearly observed as shown in Fig. 6 that the optical emission spot of Na was formed from the tip of the cone (340 μs).

3.5. Optical emission of Na observed at long distance from discharge

To enhance the explosive optical emission of Na, we used NaCl solution with a concentration of 10% as the cathode. Figure 7 shows the snapshots of phenomena when the discharge current was 120 mA and the distance between the tip of the anode and the solution surface was 10 mm. The movie file is obtainable from the supplementary data which is available at stacks.iop.org/PSST/XX/XXXXX/mmedia. (See the file of movie file spp4.mp4.) When the discharge was produced at this condition, we observed the random movement of the yellow channel. In addition, a huge number of droplets were observed around the discharge space. Figure 8 shows the result of a simple experiment which examined the spatial variation of the droplet pH around the discharge space. Litmas papers were installed around the discharge space. When the plasma was produced, droplets generated from the solution were trapped by the Litmas papers, and the color of the Litmas papers indicated the spatial distribution of pH of the droplets. As shown in Fig. 8, it was found that droplets near the plasma column were alkaline and droplets at a long distance from the plasma were acid.

4. Discussion

The aforementioned experimental results give us helpful insight into the mechanism of the droplet generation and the transport of metal atoms from the solution to the plasma. In the early stage of the discharge, we observed the perturbation on the solution surface, as shown in Fig. 6. It is considered that the change in the shape of the solution surface is induced by the electric field. It is known that the solution surface is dragged in the electric field and it becomes a conical shape which is called a Taylor cone [46–48]. In some cases, Taylor cones are observed before the breakdown [27, 39], but in the present experimental condition, we observed the formations of several cones after the ignition of the discharge. This is reasonable since the electric field in the cathode sheath is more intense than the electric field before the discharge. In general, a Taylor cone can emit droplets with small sizes from its tip. This process is utilized in the film deposition using electrospray. Therefore, it is expected that droplets of NaCl solution are emitted from the cone-shaped solution surface in the present experiment. If Na atoms are produced from the NaCl droplets in the gas phase, this can be a mechanism for the optical emission of Na in the plasma. An experimental evidence which supports this speculation is the shape of the optical emission image of Na (the firing shape from the spot on the electrolyte surface) shown in Fig. 5. The dc or a long-pulse voltage may be necessary to observe the above phenomena, since the Taylor cone is formed at several hundreds of microseconds after the ignition of the discharge. It is noted that the perturbation on the solution surface was not observed in the electrolyte-anode discharge. This is consistent with the negligible droplets and the optical emission intensity of Na. As we reported in a previous paper, we never observed optical emissions of Na in solution anode discharges even when the discharge current was higher than the experimental conditions shown in this paper [29]. We speculate that cathode sheath which has high electric field is necessary for the generations of droplets and optical emission of Na.

The experimental results also suggest another mechanism for the generation of droplets and the optical emission of Na. We propose the reaction between Na particulates and water as the second mechanism. It is well known that explosive reactions occur when solid-state alkali metals, such as Na, Li and K, arrive at water surface. The simplified reaction process is $\text{Na} + 2\text{H}_2\text{O} \rightarrow \text{H}_2 + 2\text{NaOH}$ in the case of Na as an example. The mechanism for the explosive phenomena is the fact that this reaction is highly exothermic. Recently, Mason and coworkers suggest that the early stage of the explosive phenomena is caused by the Coulomb explosion [51]. If Na atoms produced from NaCl droplets form particulates in the gas phase and they fall down to the water surface, we can expect explosive reaction which results in the generation of droplets and the optical emission of Na. This hypothesis can explain the increases in the amount of droplets (Fig. 2) and the optical emission intensities of metal atoms (Figs. 3 and 4) with the NaCl concentration. In addition, the optical emission of Na at a long distance from the discharge (Fig. 7) can also be explained by this hypothesis, since we can expect reactions between Na particulates and droplets. The color of the Litmus papers shown

in Fig. 8 indicates that the droplets at a long distance from the discharge are acid. This is reasonable since the electrolyte becomes acid in this experimental condition due to electrolysis reactions induced by the dc plasma. The detailed explanations of the electrolysis reactions are described in previous papers [32, 35]. Figure 8 also indicates that droplets near the discharge are alkaline, which is explained by the production of NaOH via $\text{Na} + 2\text{H}_2\text{O} \rightarrow \text{H}_2 + 2\text{NaOH}$.

5. Conclusions

In this work, we investigated the mechanism of the droplet generation and the optical emission of metal atoms (Na and Cu) in an atmospheric-pressure dc glow discharge employing an electrolyte cathode. The correlation between the number of droplets and the optical emission intensity indicates the importance of droplets in the transport of metal atoms from the electrolyte to the gas phase. It is considered that the production of metal atoms from droplets is the mechanism of the optical emission of metal atoms. We have proposed two mechanisms for the generation of droplets from the electrolyte cathode. The first mechanism is the distortion in the shape of the electrolyte surface by the sheath electric field. Droplets are produced from the tip of the cone-shaped electrolyte surface via a process similar to electrospray. This mechanism works for the initiation of the droplet generation in the early stage in the temporal evolution of the discharge. The second mechanism is the explosive reaction between Na particulates and water. In this mechanism, we speculate the production of Na particulates from Na atoms in the gas phase. NaCl droplets produced by the first mechanism provide Na atoms in the early stage. Once the second mechanism is switched on, the self-sustained productions Na atoms, Na particulates, and NaCl droplets are realized, resulting in the intense optical emission of metal atoms.

Acknowledgment

This work was supported by JSPS KAKENHI Grant Numbers 16H02121 and 18K03596.

References

- [1] Bruggeman P and Leys C. 2009 *J. Phys. D: Appl. Phys.* **42** 053001
- [2] Locke B R, Sato M, Sunka P, Hoffman M R. and Chang J S 2006 *Ind. Eng. Chem. Res.* **45** (2006) 882
- [3] Bruggeman P et al 2016 *Plasma Sources Sci. Technol* **25** 053002
- [4] Tabars F L 2015 *Plasma Physics and Controlled Fusion* **58** 014014
- [5] Gubkin J 1887 *Ann. Phys. (Leipzig)* **32** 114 [in German]
- [6] Davies R A and Hickling A 1952 *J. Chem. Soc.* 3595
- [7] Hickling A and Linacre J K 1954 *J. Chem. Soc.* 711
- [8] Cserfalvi T, Mezei P and Apai P 1993 *J. Phys. D: Appl. Phys.* **26** 2184
- [9] Cserfalvi T and Mezei P 1994 *J. Anal. Atom. Spectrom.* **9** 345
- [10] Cserfalvi T and Mezei P 1996 *Fresenius J. Anal. Chem.* **355** 813

- [11] Webb M R, Andrade F J, Gomez G, McCrindle R and Hieftje G M 2005 *J. Anal. At. Spectrom.* **20** 1218
- [12] Webb M R, Andrade F J and Hieftje G M 2007 *Anal. Chem.* **79** 7807
- [13] Webb M R, Andrade F J and Hieftje G M 2007 *J. Anal. Atom. Spectrom.* **22** 766
- [14] Webb M R and Hieftje G M 2009 *Anal. Chem.*, **81** 862
- [15] Bruggeman P, Liu J, Degroote J, Kong M, Vierendeels J and Leys C 2008 *J. Phys. D: Appl. Phys.* **41** 215201
- [16] Bruggeman P, Ribel E, Maslani A, Degroote J, Malesevic A, Rego R, Vierendeels J and Leys C 2008 *Plasma Sources Sci. Technol.* **17** 025012
- [17] Jenkins G, Franzke J and Manz A 2005 *Lab Chip* **5** 711
- [18] Witzke M, Rumbach P, Go V and Sankaran R M 2012 *J. Phys. D: Appl. Phys.* **45** 442001
- [19] Rumbach P, Griggs N, Sankaran R M and Go D 2014 *IEEE Trans. Plasma Sci.* **42** 2610
- [20] Chen Q, Li J and Li Y. 2015 *J. Phys. D: Appl. Phys.* **48** 424005
- [21] Mariotti D and Sankaran R M 2010 *J. Phys. D: Appl. Phys* **43** 323001
- [22] Titov V A, Shikova T G, Rybkin V V, Ageeva T A and Choi H S 2006 *High Temp. Mater. Process* **10** 467
- [23] Titov V A, Rybkin V V, Shikova T G, Ageeva T A, Golubchikov O A and Choi H S 2005 *Surf. Coat Technol.* **199** 231
- [24] Yagov V V and Getsina M L 2004 *J. Anal. Chem.* **59** 64
- [25] Yagov V V, Getsina M L and Zuev B K 2004 *J. Anal. Chem.* **59** 1037
- [26] Maximov A. I. 2007 *Contrib. Plasma Phys.* **47** 111.
- [27] Shirai N, Nakazawa M, Ibuka S and Ishii S 2009 *Jpn J. Appl. Phys.* **48** 036002
- [28] Shirai N, Ichinose K, Uchida S and Tochikubo F 2011 *Plasma Sources Sci. Technol.* **20** 034013
- [29] Shirai N, Uchida S and Tochikubo F 2014 *Plasma Sources Sci. Technol.* **23** 054010
- [30] Ishigame H, Nishiyama S and Sasaki K 2014 *Jpn J. Appl. Phys.* **54** 01AF02
- [31] Sasaki K, Ishigame H and Nishiyama S 2015 *Eur. Phys. J. Appl. Phys.* **71** 20807
- [32] Shirai N, Uchida S and Tochikubo F 2014 *Jpn. J. Appl. Phys.* **53** 046202
- [33] Shirai N, Uchida S and Tochikubo F 2017 *Jpn. J. Appl. Phys.* **56** 076201
- [34] Shirai N, Matsuda Y and Sasaki K 2018 *Appl. Phys. Express* **11** 016201
- [35] Tochikubo F, Shirai N, Uchida S 2014 *Jpn. J. Appl. Phys.* **53** 126201
- [36] Yamazaki Y, Shirai N, Nakagawa Y, Uchida S, Tochukugo F 2018 *Jpn. J. Appl. Phys.* **57** 096201
- [37] Urabe K, Shirai N, Tomita K, Akiyama T and Murakami T 2016 *Plasma Sources Sci. Technol.* **25** 045004
- [38] Sirotkin N A, Titov V A 2017 *Plasma Chem. Plasma Process.* **37** 1475.
- [39] Schwartz A J, Ray S J, Elish E, Storey A P, Rubinshtein A A, Chan G C Y, Pfeuffer K P and Hieftje G M 2012 *Talanta* **102** 26
- [40] Greda K, Jamroz P, Dzimitrowicz A and Pohl P J 2015: *Anal. At. Spectrom.* **30** 154
- [41] Jamroz P, Greda K and Pohl P 2012 *TrAC Trends Anal. Chem.* **41** 105
- [42] Greda K, Jamroz P and Pohl P 2013 *J. Anal. At. Spectrom.* **28** 1233
- [43] Jamroz P, Zyrnicki W and Pohl P 2012 *Spectrochim. Acta, Part B* **73** 26
- [44] Greda K, Swiderski K, Jamroz P and Pohl P 2016 *Anal. Chem.* **88** 8812
- [45] Evans E H and Giglio J J 1993 *J. Anal. At. Spectrom.* **8** 1
- [46] Taylor G 1964 *Proc. R. Soc. London, Ser. A* **280** 383
- [47] Zeleny J 1917 *Phys. Rev.* **10** 1
- [48] Zeleny J 1914 *Phys. Rev.* **3** 69
- [49] Mason P E, Uhlig F, Van 嫻 V, Buttersack T, Bauerecker S and Jungwirth P. 2015 *Nature Chemistry* **7** 250

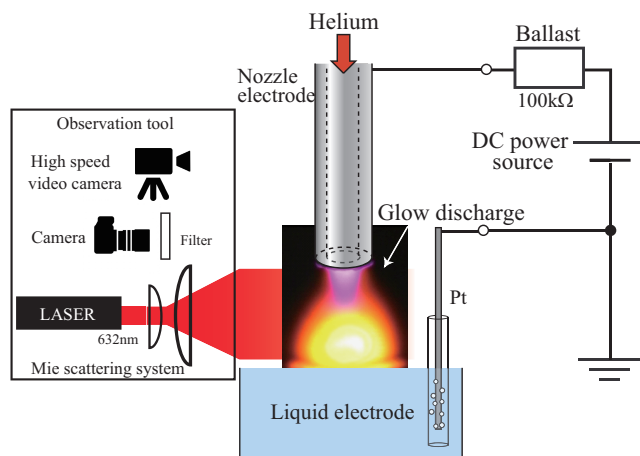


Figure 1. Experimental setup

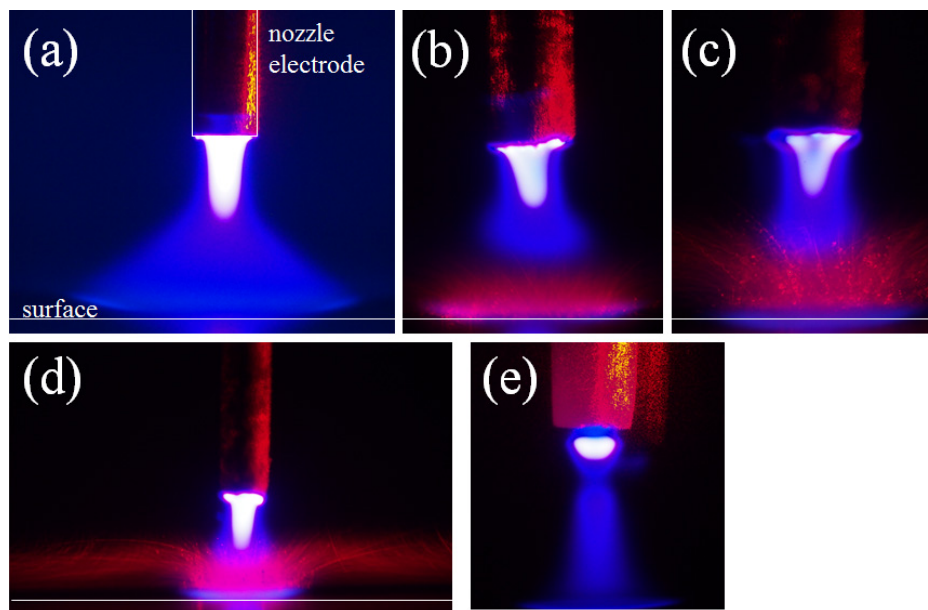


Figure 2. Visualization of droplet generation from liquid cathode surface by laser Mie scattering. (a) tap water, discharge current: 90 mA, (b) 1% NaCl solution, discharge current: 90 mA (c) 5% NaCl solution, discharge current: 90 mA (d) zoom out image of (c), and (e) liquid anode (1% NaCl solution) discharge at discharge current of 30 mA. Movie files as supplementary data are available from stacks.iop.org/PSST/XX/XXXXX/mmedia (See the movie file spp1.mp4).

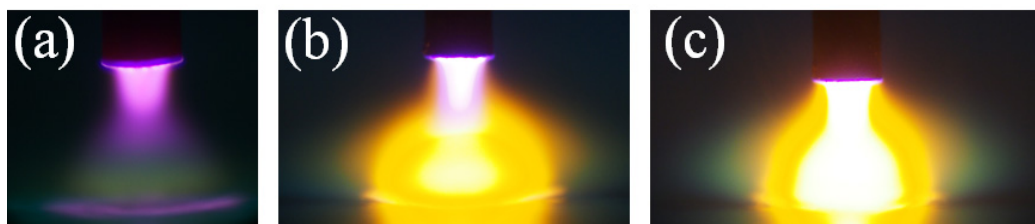


Figure 3. Discharge images when CuSO_4 solutions at a concentration of 2.8% were used as the cathode. The concentrations of NaCl additive were (a) 0%, (b) 1%, and (c) 2.8%. The discharge current was 90 mA.

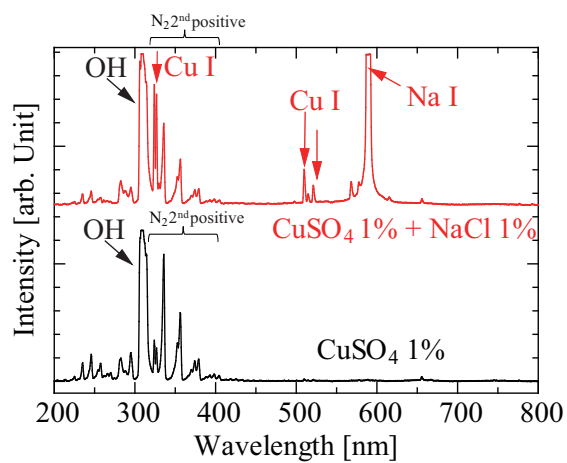


Figure 4. Optical emission spectra when CuSO_4 solutions at a concentration of 1% were used as the cathode. The lower trace was observed without the NaCl additive. The optical emission intensity of Cu was enhanced by adding 1% NaCl as shown in the upper trace. The discharge current was 90 mA.

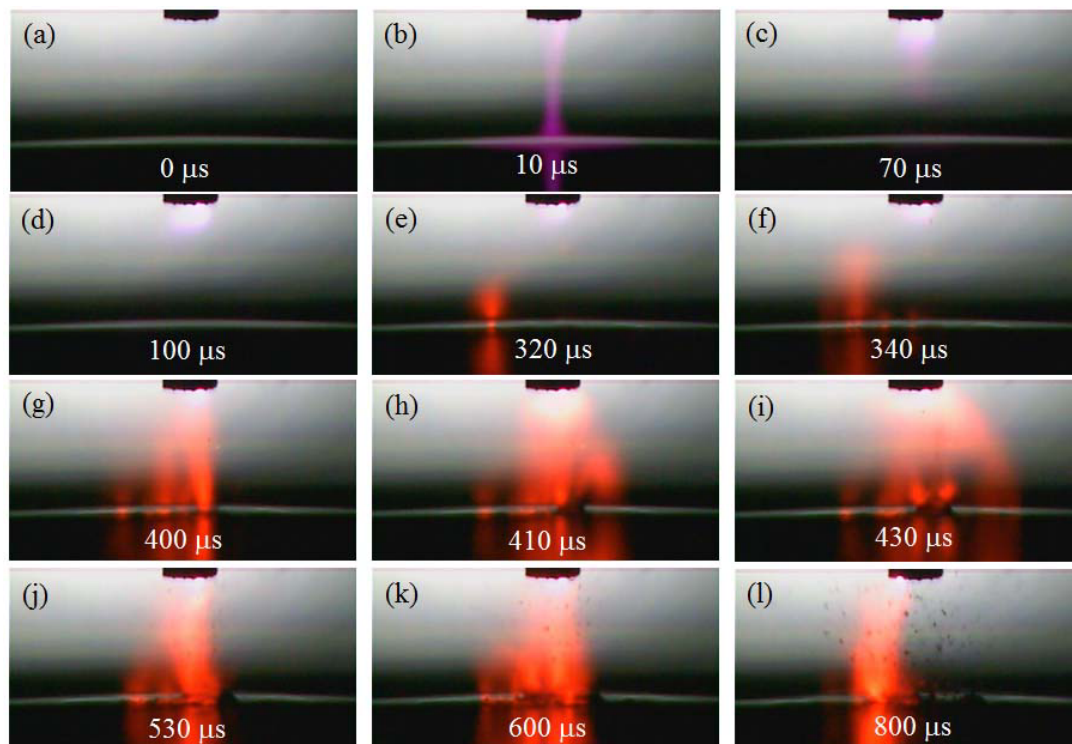


Figure 5. Time evolution of the optical emission of Na on the cathode surface when an atmospheric-pressure glow discharge with a liquid cathode is ignited. The frame rate of high-speed camera is 10^5 fps. * Movie files as supplementary data are available from stacks.iop.org/PSST/XX/XXXXX/mmedia. (See the movie file spp2.mp4).

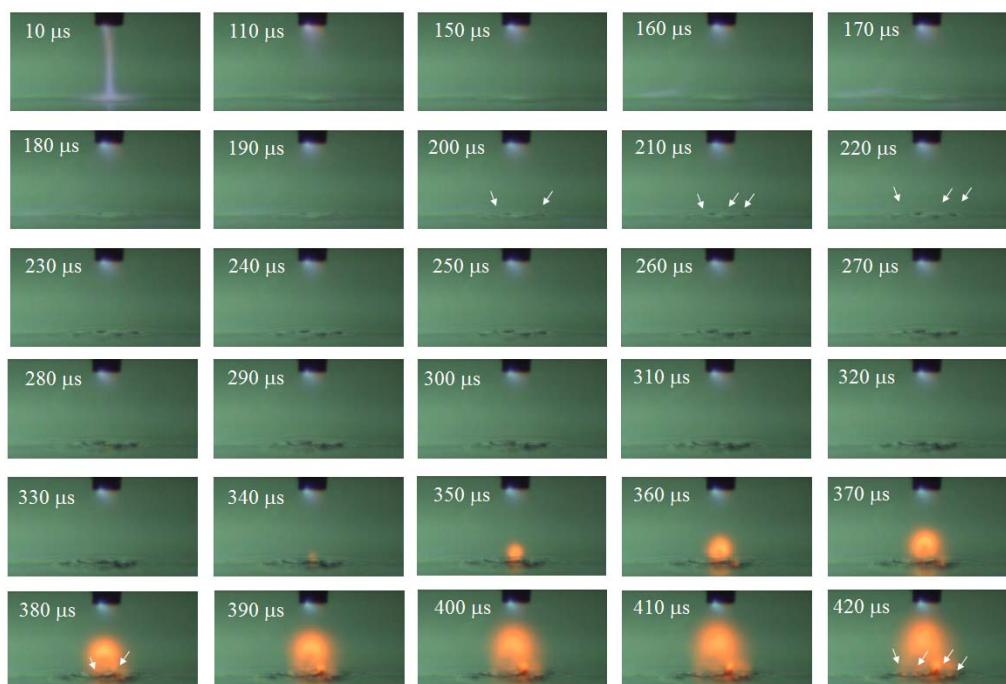


Figure 6. Temporal change in the shape of the liquid cathode surface. The frame rate of high-speed camera is 10^5 fps. Supplementary data are available from stacks.iop.org/PSST/XX/XXXXX/mmedia. (See the movie file spp3.mp4).

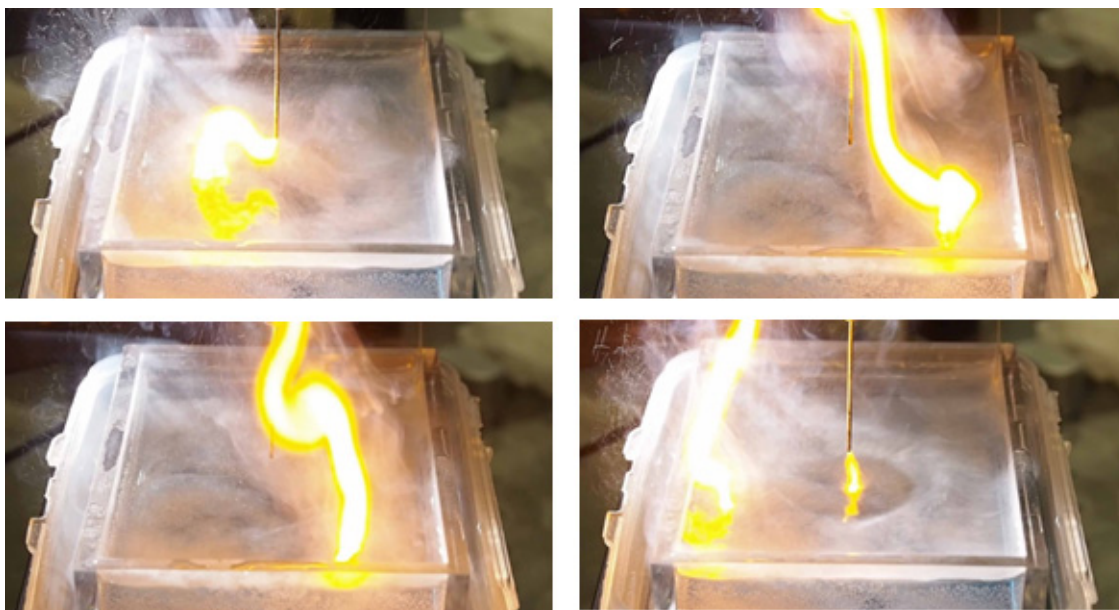


Figure 7. Explosive phenomena observed above the liquid cathode when the distance between the anode and the cathode surface was 10 mm and the discharge current was 120 mA. *Supplementary data are available from stacks.iop.org/PSST/XX/XXXXX/mmedia (See the movie file spp4.mp4).

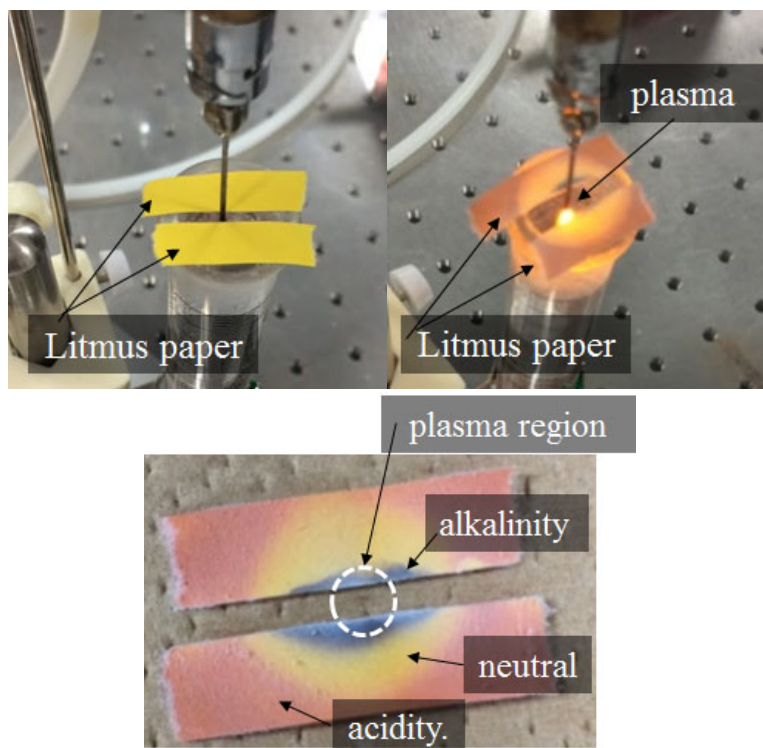


Figure 8. Radial distribution of the pH value of droplets examined using Litmus papers.